

# In situ measurement of fractal dimension using focussed beam reflectance measurement<sup>☆</sup>

Peter Kovalsky<sup>\*</sup>, Graeme Bushell

*School of Chemical Engineering and Industrial Chemistry, The University of New South Wales, Sydney, NSW 2052, Australia*

## Abstract

Focussed beam reflectance measurement is a technique that shows some promise as a technique for the online characterisation of floc size and structure. A scanning laser is focused into process fluid and the reflected intensity is measured as a function of time. This light intensity signal is normally processed to return chord length measurements which contain combined information on particle size and shape.

This study shows that the unprocessed signal can be expected to encode information about the texture of the particle being scanned in addition to size and shape. For the purpose of characterising floc structure, a power law exponent can be recovered from the Fourier transform of the unprocessed signal and this in turn is related to the mass fractal dimension of flocs.

The technique is demonstrated with computer generated flocs and with flocculated polystyrene latex of a primary particle size of 5  $\mu\text{m}$  and a mass fractal dimension of  $D_m = 2.5$  as determined by the volume obscuration method.

Results obtained through simulation studies into scanning of computer generated flocs demonstrate that a correlation exists between the power law exponent and the mass fractal dimension. Loose structures with mass fractal dimension of  $D_m = 1.64$  returned a power law exponent of  $\beta = -1.77$  whilst a tighter structure of mass fractal dimension of  $D_m = 2.34$  returned a power law exponent of  $\beta = -1.92$ .

Results obtained through scanning of polystyrene latex flocs of mass fractal dimension of  $D_m = 2.49$  returned a power law exponent of  $\beta = -2.00$  which appears not to be in quantitative agreement with the simulation results.

© 2005 Elsevier B.V. All rights reserved.

**Keywords:** Reflectance; Floc; Polystyrene latex

## 1. Introduction

The process of aggregation is fundamental to improving the operation of solid–liquid separation processes such as sedimentation, thickening, flotation and filtration. The hydrodynamic properties of aggregates relative to their primary particles are the driving force for these processes. For example, in sedimentation, an aggregate brought together by a large grouping of primary particles will settle much faster than a dispersion of primary particles, hence providing a faster rate of separation.

Common applications of aggregation are typically stages in the area of effluent treatment from mineral processing and municipal waste. More recently, there has been considerable

interest in adjusting aggregation conditions in order to fine tune the physical properties of aggregates to suit a specific application. For example, in low pressure membrane filtration, aggregates of loose (porous) structure are preferred as their structural properties in suspension are thought to retain their permeable structure when deposited as a cake on a membrane allowing for higher flux rates to be achieved over a longer period of time [1]. On the other hand, many people believe that compact flocs are preferable in sedimentation thickeners as their structures form sludge that are relatively low in moisture content, thus easier to transport and dispose of. Floc characterization techniques can play a vital role in reporting the relevant physical parameters to improve separation efficiency of these processes through improved control of floc properties.

Characterization of floc structure is fundamentally based on the spatial arrangement and the number of particles within the structure. Physical properties of floc such as porosity, permeability, density, floc size and floc structure can be expected

<sup>☆</sup> EIC Conference on Solid–Liquid Separation IV, Pucon, Chile, December 2003.

<sup>\*</sup> Corresponding author. Tel.: +61 2 9385 4367; fax: +61 2 9385 5966.  
E-mail address: peter.kovalsky@student.unsw.edu.au (P. Kovalsky).

to be important parameters in the design of industrial equipment for a particular application.

One macroscopic approach to quantitatively characterize the complex structure of flocs is known as the mass fractal dimension, first demonstrated by Forrester and Witten [2]. The mass fractal dimension is defined as

$$M \propto R^{D_m} \quad (1)$$

where  $M$  is the mass of the particles,  $R$  the linear measure of size and  $D_m$  is the mass fractal dimension. The fractal dimension of a floc gives practical information related to porosity, permeability, density and structure. Values of  $D_m$  are always between 1 (linear string of particles) and 3 (a compact space-filling structure). Putting the concept of fractal dimension into geometrical context is best illustrated through structural comparison of computer generated flocs shown in Fig. 1.

There are a number of techniques, which have been developed to measure the structure of flocs in terms of mass fractal dimension, summarized by Bushell et al. [3]. These include techniques based on small angle light scattering, image analysis and hydrodynamic settling tests. The major drawbacks to these techniques are their limited practicality towards industrial applications. This is mainly due to portability and robustness issues. A further drawback is that the measurements required to apply these correlations become difficult at high solids concentrations.

The Lasentec focused beam reflectance measurement (FBRM) is marketed as an in situ tool for sensing changes to size and shape of suspended solids in a general sense. The nominal range of solids concentration upon which most particle sizing instruments operate is typically quite narrow which is quite acceptable under laboratory conditions but not suitable for in situ measurement. In comparison, FBRM is capable of operating over a wide range of solids concentrations from very dilute up to slurry type mixtures. This property alone gives it considerable appeal for being adapted for use as a floc characterization tool, most particularly for industrial applications where solids concentrations of process fluids can be quite broad.

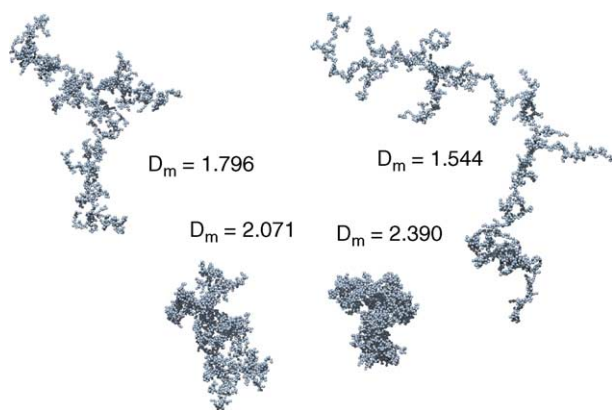


Fig. 1. Variety of computer generated floc structures ranging from loose ( $D_f = 1.544$ ) to compact ( $D_f = 2.390$ ).

The FBRM (model M400L-316K) consists of a laser scanning at a fixed high velocity (2 m/s) housed in a rigid stainless steel probe, which is inserted into a solid suspension. A spinning lens is used to generate the circular path tracked by the laser, which is achieved through precise optical reflection and beam splitting. Ordinarily the light reflected back off the suspended particles is collected and passed back to the electronics where chord length is calculated based on duration of a high reflectance signal. The data are collected and reported as a chord length distribution.

The experimental work described here details the extension of the capabilities of the FBRM to extract information about floc structure based on spectral analysis of the reflected laser signal. Simulation of floc laser scanning has been used to assist with developing an understanding of this system, and subsequently to extract structural information from the real FBRM raw signal.

## 2. Simulation

The approach taken to modeling the modified FBRM system was based on the analysis of a large pool of generated floc images of various structures. A flow diagram of the analysis is presented in Fig. 2 showing the sequence of steps used in obtaining simulated FBRM scans of flocs and further processing required to extract structural information.

Floc structures were generated based on an algorithm similar to that described by Thouy and Jullien [4]. The simulations produced a list of 3D-cartesian coordinates of primary particles, which make up the floc structure. A tunable parameter was presented to the algorithm such that a number of structures generated ranging from a  $D_m = 1.54$ –2.39. This process of simulated cluster–cluster aggregation was created through modeled collision and sticking of primary particles at first, continuing to form progressively larger flocs, which are returned to the list. Control of the structure being formed was enabled by a rule that specified the sticking of cluster to cluster during aggregate growth based on the level of interpenetration of the aggregates.

Floc images are prepared from particle coordinates data using a layered approach with the image data conditioned such that simulated laser scanning can be performed. Each primary particle was plotted as a  $5 \mu\text{m}$  sphere in sorted order from furthest to nearest on the image giving the impression of an orthographic representation of a floc. This technique was tuned for rapid simulation of pools of large flocs consisting of up to 10,000 primary particles in each.

The brightness of each image pixel was determined by an optical scanning model, representing the reflected laser intensity profile off each primary particle. The optical scanning model simply predicts the normalized light flux received through spherical particle reflection at a detector positioned at  $180^\circ$  to the emitted laser. The received intensity is based on specular and diffusive reflection (Fig. 3) as a function of position on the primary particle sphere. In this case, a pixel

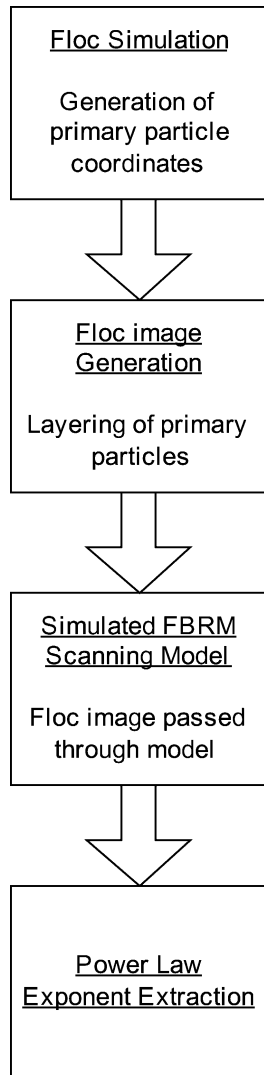


Fig. 2. Flow diagram of simulation.

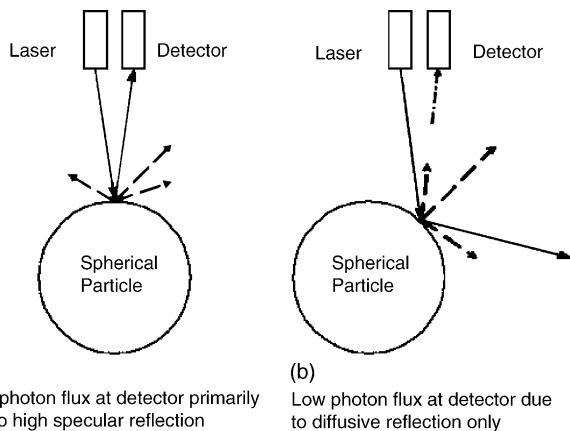


Fig. 3. (a) Pictured left, indicates high laser reflectance resulting from specular reflectance (solid line) and (b) right, indicates low reflectance comprising entirely of diffusive reflectance (dashed line).

has a dimension of  $1\ \mu\text{m} \times 1\ \mu\text{m}$ , which is a conservative estimate of the FBRM laser spot size specification based on the instruments capability to resolve particle chord lengths down to  $1\ \mu\text{m}$ .

A simulated raw signal, which is proposed to contain information about floc structure, is created through taking linear scans, shown in Fig. 4. With the image data stored in matrix form this task are as simple as taking a row vector from this matrix. Each entry in this vector array corresponds to the brightness of the pixel in the scanning path in order. Performing the scan in this way with the parameters described essentially simulates sampling at one sample per micron along the laser path. With the laser tracking at 2 m/s, this corresponds to a real world sampling frequency of 2 MHz.

Several scans were performed on each floc at different sections along its length to simulate a floc moving at constant velocity through the laser focal plane shown in Fig. 5. A long array containing many scans was generated by taking scans from evenly spaced rows and joining the individual vectors end to end to form a single large vector for spectral analysis. In this process, only the structural content (i.e. peaks within the floc chord) of the individual vectors are cut and joined with baseline signal omitted. This was performed to reduce spectral bias from polydisperse chord distributions, which was expected to be present in real scanning. The conditioned array that contains structural information only is referred to as the reflected intensity profile.

The power law extraction technique involves spectral analysis of the reflected intensity profile. This was performed through fast fourier transform (FFT) over the length of the intensity profile vector to extract structural information encoded in the signal. This concept is adapted from works performed in other areas such as machined surface characterization [5–7] and cardiology to investigate the fractal nature of electrocardiographs [8].

The power spectral density profile is obtained by the following equation:

$$\text{power spectral density} = |\text{FFT}(f)|^2 \quad (2)$$

where  $|\text{FFT}(f)|$  is the magnitude of the spectral content at frequency ( $f$ ) obtained by fast fourier transform of the reflected intensity profile. This analysis is performed between 0 and  $F_s/2$  (Hz) where  $F_s$  is denoted as the sampling frequency. The power spectral density profile is typically power law between 0 and  $F_s/2$  with the power law exponent denoted as  $\beta$ , proposed to give an indication of the structure of the flocs being scanned as shown in Fig. 6.

### 3. Simulation results

Simulation was performed on floc structures ranging from  $D_m = 1.54\text{--}2.39$ . The power law exponent was extracted using spectral analysis, the mean results of which are plotted in Fig. 7.

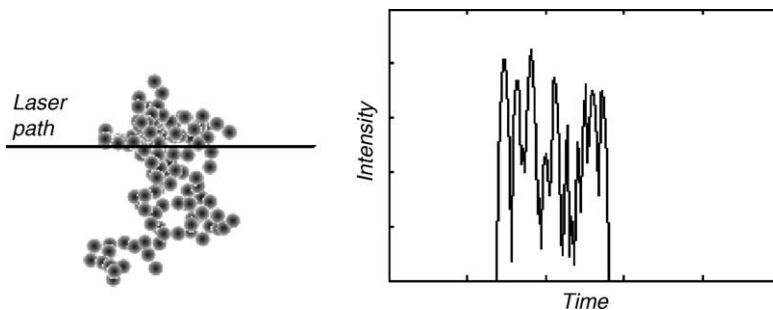


Fig. 4. Illustrates the expected reflected intensity off the surface of a computer simulated floc.

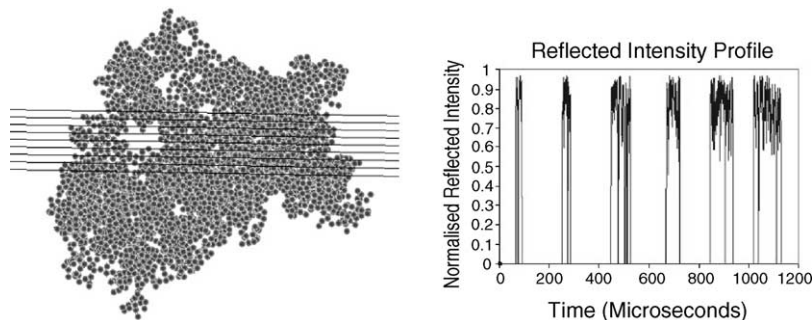


Fig. 5. Diagram illustrating multiple scans (left) and the corresponding array (right) obtained through joining scans (prior to omitting dead signal). The figure thus illustrates a simulated FBRM reflected intensity profile obtained through scanning of a floc.

Fig. 7 illustrates a correlation between the power law exponent and mass fractal dimension. The sensitivity of this trend to simulation parameters such as floc size and floc velocity was low for these changes indicating that the model would be reasonable for real scanning data.

#### 4. Experimental

A real flocculating system was setup to validate the simulation results. This system consisted of flocculated polystyrene latex spheres aggregated with  $MgCl_2$  and polymeric floccu-

lant. The aim of experiments was to verify a relationship between floc structure and FBRM power law exponent through scanning of a real floc system such as polystyrene latex. In these experiments, the floc structure was reported as the mass fractal dimension, which was determined using the volume obscuration technique [9,10] by a Coulter LS230 (small angle light scattering). The aim of configuring the apparatus in this experiment is to obtain consistent particle structure analysis at the instrument/sample interfaces in this experiment. The experimental rig consists of a Coulter LS230 particle size analyser and a modified FBRM with tubing connected between instruments and a peristaltic pump to drive the fluid through the process as shown in Fig. 8. Key to the consistency of results is protection of the developing flocs from shear damage as a result of pumping and turbulence. To reduce the

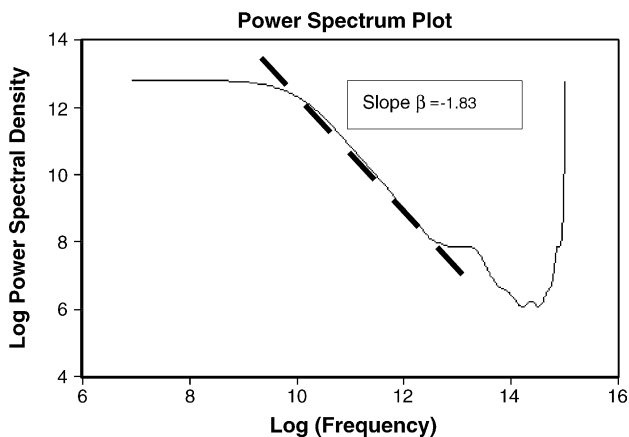


Fig. 6. Power spectrum analysis of a simulated signal for a floc of fractal dimension of  $D_f = 1.79$ . The slopes appear to be different for each floc structure.

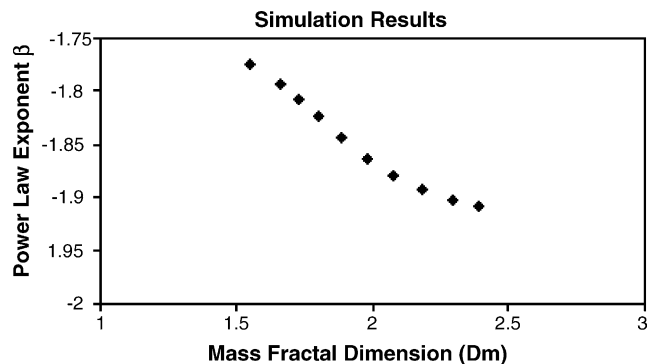


Fig. 7. Plot of power law exponent vs. fractal dimension of various floc structures.

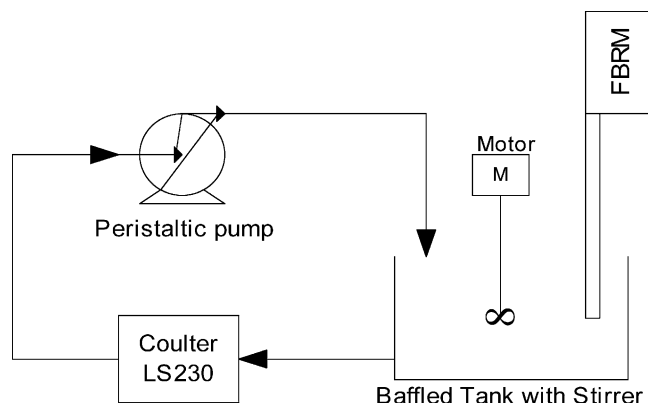


Fig. 8. Closed circuit experimental setup.

extent of shear in the system the fluid is gravity driven by an elevated stirring vessel with pumping introduced at the final point in the closed circuit.

Other key considerations are to create a system where flocs of considerable size can be presented to the FBRM probe. This is controlled through choice of solution chemistry such as divalent salt concentration and polymeric flocculant to enhance growth of flocs.

Fig. 8 illustrates the experimental setup. Polystyrene latex and coagulants are added to the elevated baffled tank, which is essentially a mixing vessel. A shear environment is introduced through an axial flow impeller placed in the tank with shearing rates set to give orthokinetic aggregation. Polymeric flocculant Zetag 7642 was dosed to a solution of 0.25 M  $MgCl_2$  and 0.005 g/100 ml polystyrene latex corresponding to a volume obscuration of 20% with the entire system totalling 1.5 l. The Zetag flocculant dosage used in the system was 2  $\mu\text{g/l}$ . The polystyrene latex used in this experiment was a negatively charged, surfactant free, sulphate white polystyrene latex. The mean diameter determined from transmission electron microscopy was 4.9  $\mu\text{m}$  with a standard deviation of 0.30  $\mu\text{m}$ . The polystyrene latex was supplied by

Interfacial Dynamics Corporation (IDC) delivered in distilled de-ionized water at a concentration of 4.1 g/100 ml. The density of the polystyrene at 20 °C was 1.055 g/cm<sup>3</sup>.

Prior to analysis, the FBRM focal position was adjusted to obtain the optimum reflected optical signal possible. This was done to ensure the highest resolution was obtained at the data acquisition stage. A focal length of 3.2 mm was selected by adjusting the focal position from zero through to the optimum setting. This procedure was monitored by placing the probe in a suspension of latex and observing the average signal peak intensity on a PC oscilloscope from the TIA500 optical to electrical converter.

Reflected laser scanning data were then acquired through the FBRM, which was positioned in the vessel near the out-flow port. The FBRM, when used normally with the Lasentec data logging hardware, measures and records chord length distribution of a particulate system. The optical connection, otherwise routed to the Lasentec hardware was rerouted to a TIA500 optical to electrical converter for alternate analysis. Extraction of the power law exponent from the raw FBRM optical signal involved high speed integration of optical to electrical signal conversion, data logging hardware and spectral analysis software shown in Fig. 9. The data acquisition hardware specifications such as bandwidth (125 MHz) and settling time were selected such that response dynamics were expected to have negligible effects in the working size range (above 1  $\mu\text{m}$ ).

Suspended flocs grown in the mixing vessel flow under gravity through the Coulter LS230 small angle light scattering instrument for volume obscuration analysis before being pumped as return to the mixing vessel. The volume obscuration method for characterizing floc structure provides an estimate of the mass fractal dimension  $D_m$  [9,10] based on parameters such as volume obscuration and  $D(4, 3)$  mean diameter, both reported by the Coulter LS230. The principle is based on a modeled trend of a decrease in projected area by the solids that were observed by the Coulter detectors during latex floc growth.

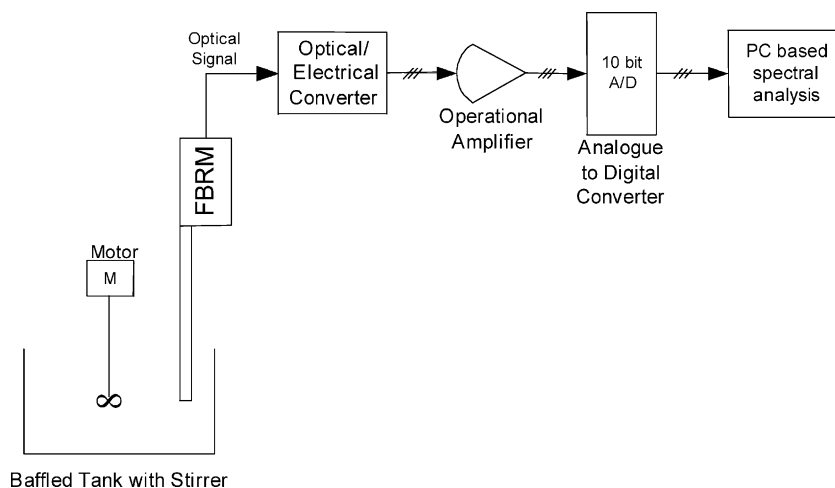


Fig. 9. Hardware configuration used to convert and acquire optical scanning data.

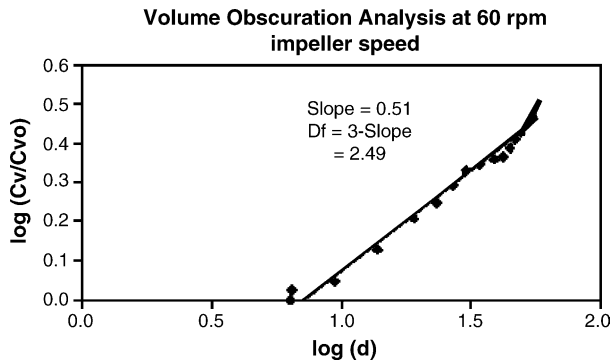


Fig. 10. Volume obscuration analysis to determine floc mass fractal dimension for latex flocs at an impeller speed of 60 rpm.  $C_v/C_{v0}$  is the ratio of suspended solids volume fraction to initial solids volume fraction calculated from volume obscuration as reported by the Coulter LS230. Particle diameter  $D(4, 3)$  is given in microns as reported by the Coulter LS230.

## 5. Results and discussion

Our volume obscuration analysis showed that a reproducible latex floc structure with a fractal dimension of  $D_m = 2.49 \pm 0.09$ , as reported by volume obscuration model fitting as shown in Fig. 10, suggesting that this parameter could be measured with confidence with the closed loop experimental configuration. The final floc structure was independent of shear rate in the baffled tank for the 60, 120 and 450 rpm impeller speeds.

The results displayed by Fig. 11 shows that the experimental and simulation ranges do not overlap but it appears the results between the two are inconsistent. The most readily recognizable difference between the simulated and experimental scans was the unavoidable presence of noise in the experimental data logging hardware. The effect of noise on the results obtained through spectral analysis is quite difficult to assess based on visual examination of scans as shown in Fig. 12.

As introduced earlier, a simplistic spherical optical reflection model was assumed and applied in the simulation model with the aim that this simplified model could reasonably recreate floc morphological features upon simulated scan-

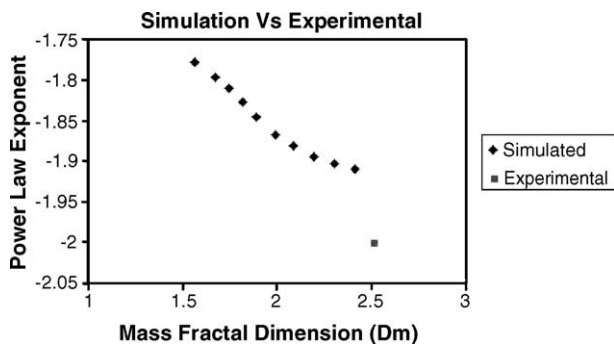


Fig. 11. Comparison between results obtained for simulation and experimental scanning of polystyrene latex flocs. Mean floc diameter  $D(4, 3)$  was approximately  $100 \mu\text{m}$  as determined by light scattering.

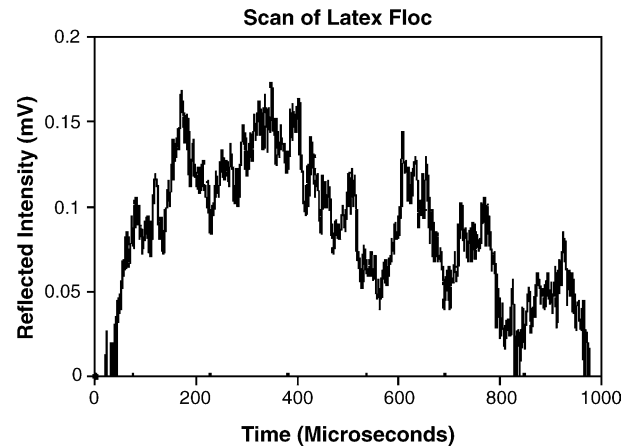


Fig. 12. Real latex floc scan. Sampled floc chord length is approximately  $1000 \mu\text{m}$ .

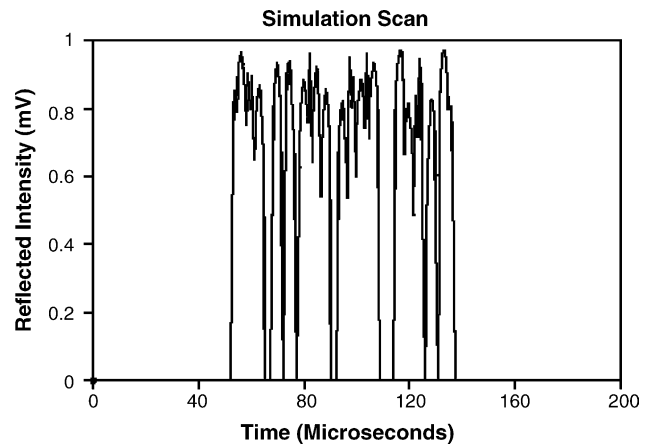


Fig. 13. Typical simulation scan of a floc.

ning. A correlation between the power law exponent and the fractal dimension was demonstrated indicating that simple scanning and analysis does recover structural information. However, the experimental results suggest that the model

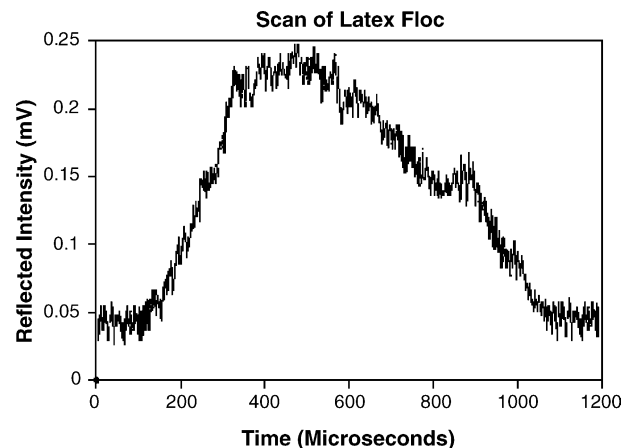


Fig. 14. Real scan of zirconia floc. Sampled floc chord length is approximately  $800 \mu\text{m}$ .

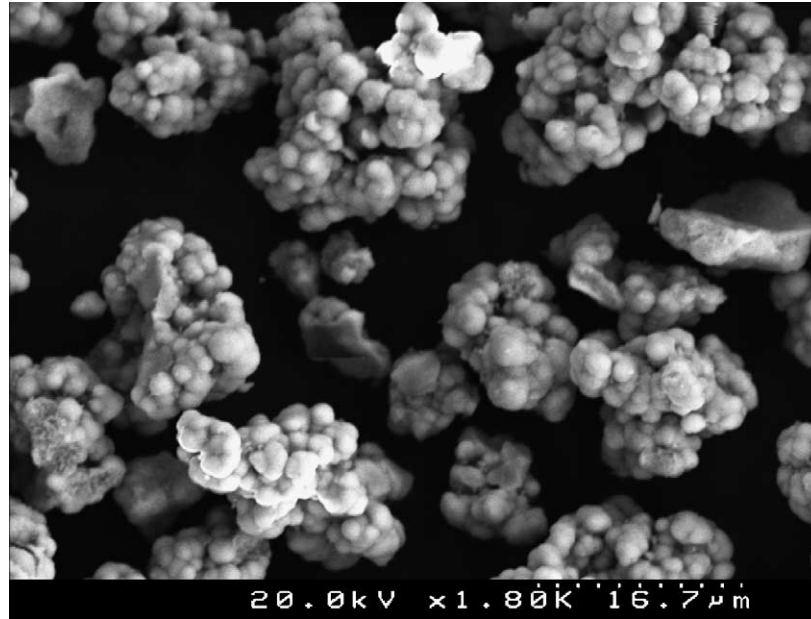


Fig. 15. Scanning electron microscope image of zirconia flocs illustrating their compact structure.

used in image generation component of the simulation falls well short of describing the true optical characteristics of polystyrene latex aggregates. This can be verified through direct comparison of simulation and experimental scans (see Figs. 12 and 13) and is probably the reason why there is a difference in the results of analysis.

The presence of noise in the experimental signal is evident and undoubtedly would have a detrimental effect on the recoverability of structural information through spectral analysis. At this stage, it would be quite difficult to conclude

that the presence of noise alone accounts for the difference between real and simulated scanning without further investigation and experiments. Another possibly more serious issue is that the real laser is focussed at a narrow point whereas the simulated one is a thin beam. This implies that the optical model used in simulation fails to account for sensitivity to scanning depth into the floc structure. Further modelling investigations would account for both noise and depth sensitivity to attempt to validate the simulation results with what is observed experimentally.

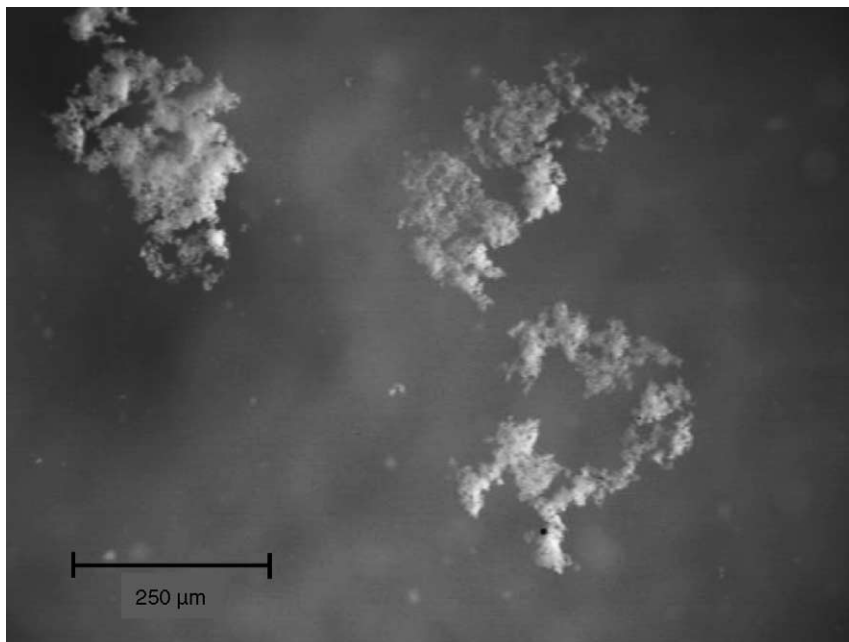


Fig. 16. Leica microscope image of latex flocs illustrating their loose structure.

Experimental FBRM scanning does indicate that the raw reflectance signal contains structural information. This can be demonstrated through comparison of results from two different floc systems, latex and zirconia. Fig. 14 illustrates a typical real scan of a zirconia floc in suspension aggregated with polymeric flocculant. Comparison with Fig. 12 shows that the zirconia floc exhibits smoother long-range structure suggesting that a more compact floc is being scanned. Scanning electron microscope images of zirconia flocs (see Fig. 15) validate this observation, which shows compact flocs. In comparison, images of latex flocs are taken with a Leica microscope (see Fig. 16) showed a relatively loose structure.

## 6. Recommendations

The model used in simulation falls well short of describing the true optical characteristics of polystyrene latex aggregates. This can be visually verified through direct comparison of real and experimental scans and is fundamentally the reason why there is a difference in the results of analysis. To address this, several areas need to be considered to further prove the viability of this technique. Primarily, this work would focus on a more sophisticated Monte Carlo simulation to reflect a more realistic floc scan, which would be used to further develop our model. Additions to the simulation would include a incorporation of a distance factor into the pixel intensity model and superimposed noise onto the reflected intensity profile. This would ultimately assist in developing the spectral analysis technique to be applicable to real systems.

Further experiments will focus on the use of other flocculants to grow the monodisperse latex spheres into large, low  $D_f$  structures.

## 7. Conclusion

A simplistic model, based around a proposed modification of the FBRM, was used to simulate the scanning of polystyrene latex spheres with particular interest in extracting structural information encoded in the raw reflectance signal through spectral analysis. From this model a correlation between the mean power law exponent for several computer generated floc structures was demonstrated under simulated scanning. It was possible to modify the FBRM through a relatively simple integration of data logging hardware and optical/electrical conversion to extract equivalent real data. Polystyrene latex flocs were grown and the structure analyzed

using volume obscuration analysis. Analyzing the spectral content of the real reflected FBRM signal for the latex system showed that there is a clear difference between simulation and experimental results. A fractal dimension of  $D_m = 2.49$  was reported with a power law exponent of  $\beta = -2.00$  measured falling outside the simulated trend. The presence of unavoidable noise in the electrical hardware is believed to have had a detrimental effect on the recoverability of structural information through spectral analysis which could explain the difference between experimental and simulation results. However, despite the inadequacy of the model developed through simulation, experimental FBRM scanning does indicate that the raw reflectance signal contains structural information and this was demonstrated through direct visual comparison of scans of loose latex flocs and compact zirconia flocs which is verified against microscopic imaging. This suggests that a rigorous model taking into account the deficiencies of the current approach will be able to quantitatively resolve the difference between flocs of different structure and thus will be the focus of future work.

## References

- [1] T.D. Waite, A. Schaefer, A.J. Fane, A. Heuer, Colloidal fouling of ultrafiltration membranes: impact of aggregate structure and size, *J. Colloid Interface Sci.* 212 (1999) 264–274.
- [2] S.R. Forrest, T.A. Witten Jr., Long-range correlations in smoke-particle aggregates, *Phys. A* 12 (1979) 109–117.
- [3] G.C. Bushell, Y.D. Yan, D. Woodfield, J. Raper, R. Amal, On techniques for the measurement of the mass fractal dimension of aggregates, *Adv. Colloid Interface Sci.* 95 (1) (2002) 1–50.
- [4] R. Thouy, R. Jullien, Structure factors for fractal aggregates built off-lattice with tunable fractal dimension, *J. Phys. I* 6 (1996) 1365–1376 (France).
- [5] C.Q. Yuan, J. Li, X.P. Yan, Z. Peng, The use of the fractal description to characterize engineering surfaces and wear particles, *Wear* 255 (1–6) (2003) 315–326.
- [6] M. Hasegawa, J. Liu, K. Okuda, M. Nunobiki, Calculation of the fractal dimensions of machined surface profiles, *Wear* 192 (1–2) (1996) 40–45.
- [7] Z. Jiang, H. Wang, B. Fei, Research into the application of fractal geometry in characterising machined surfaces, *Int. J. Machine Tools Manuf.* 41 (13–14) (2001) 2179–2185.
- [8] P.B. DePetrillo, A. Speersb, U.E. Ruttimann, Determining the Hurst exponent of fractal time series and its application to electrocardiographic analysis, *Comput. Biol. Med.* 29 (1999) 393–406.
- [9] P.T. Spicer, S.E. Pratsinis, J. Raper, R. Amal, G. Bushell, G. Meesters, Effect of shear schedule on particle size, density, and structure during flocculation in stirred tanks, *Powder Technol.* 97 (1) (1998) 26–34.
- [10] T. Serra, X. Casamitjana, Structure of the aggregates during the process of aggregation and breakup under a shear flow, *J. Colloid Interface Sci.* 206 (1998) 505–511.